Displacement Defect Formation in Complex Oxide Crystals under Irradiation

S.B. Ubizskii[1]) (a), A.O. Matkovskii (a, b), N. Mironova-Ulmane (c), V. Skvortsova (c), A. Suchocki (d), Y.A. Zhydachevskii (a), and P. Potera (b)

(a) State University Lviv Polytechnic, 12 Bandera St., 79646 Lviv, Ukraine

(b) Institute of Physics HPS, 16A Rejtana St., PL-35-310 Rzeszow, Poland

(c) Institute of Solid State Physics, University of Latvia, 8 Kengaraga St., LV-1063 Riga, Latvia

(d) Institute of Physics, PAS, 32/46 Al. Lotnikow, PL-02-668, Warsaw, Poland

The work is devoted to an analysis of formation processes of the radiation displacement defects (RDDs) and colour centres (CCs) in complex oxide crystals under irradiation. The calculation results on the displacement process simulation as well as an analysis of the RDD and CC accumulation kinetics are presented. New experimental results on additional absorption spectra induced by neutron irradiation of $LiNbO_3$ (LNO) crystals doped with Fe and Cr and $YAlO_3$ (YAP) crystals doped with Nd and Er as well are presented. Dose dependencies of the additional absorption are compared and their peculiarities are discussed. The obtained results confirm that CCs causing the irradiation induced absorption in LNO and YAP crystals are formed in secondary processes which are affected by impurities. It is also found that the induced absorption dose dependence in LNO crystals has an unexpected slope.

1. Introduction

During irradiation of crystals the radiation energy is mainly dissipated on excitation of the electron subsystem of the crystal, i.e. on ionizing of matter. Ionisation processes may lead to changing of the charge state of genetic defects and formation of metastable defect centres including colour centres (CC). Recharging of genetic defects with increase of irradiation dose is limited by the defect quantity and by an inverse process of centre destroying.

An insignificant part of the radiation energy is lost in elastic collisions of radiation particles or secondary ones with crystal atoms. If the energy transmitted to an atom during the elastic scattering exceeds the threshold displacement energy, then the Frenkel pair may be created. This model is known as the impact mechanism of RDD formation. These defects as well as genetic defects may recharge under the ionizing influence of radiation that leads to the creation of new defect centres. Unlike the genetic defect recharging this process is not limited by the defect quantity, as the latter one increases with a radiation dose. Nevertheless, the accumulation of radiation defects and colour

---

[1]) Correspondence address: Department of Semiconductor Electronics, State University Lviv Polytechnic, 12 Bandera St., 79646 Lviv, Ukraine; Tel.: (380)-(322)-398153, Fax: (380)-(322)-742164, e-mail: granat@carat.lviv.ua

centres on them may be limited by annihilation processes of the components of Frenkel pairs when one of them finds itself in the annihilation zone of another one.

There are many literature experimental data devoted to the influence of ionizing radiation on oxide crystals (e.g. see monographs [1 to 3]). Most of literature data are dedicated to investigation of CC formation under UV-light, X-ray and γ-irradiation influence and investigation of their nature. Much less of them are devoted to irradiation by high energy electrons and fast neutrons that result in the displacement defect formation. Among the important in practical sense and well-known complex oxide crystals only for a few of them there are enough experimental data. Let us remind shortly the main peculiarities revealed in some complex oxides at high-energy irradiation.

$Y_3Al_5O_{12}$ The influence of fast reactor neutrons and the high energy electron irradiation on yttrium aluminium garnet (YAG) single crystals (pure and rare-earth element doped) was investigated in many works [4 to 15]. While the additional absorption (AA) bands induced by γ-quanta irradiation saturate at 10^3 to 10^5 Gy absorbed doses [1, 6, 16], in the case of electron irradiation with energy of 5 MeV the absorption band peaked at 390 nm does not exhibit any saturation tendency at fluences up to 10^{19} cm^{-2} ($\sim 2 \times 10^9$ Gy absorbed dose) [10, 14]. These optical changes in YAG crystals as well as similar changes after the 50 MeV electron irradiation [10] are explained by radiation displacement defect formation. The YAG crystal coloration induced by neutron irradiation increases monotonously too within the fluence range of 10^{16} to 10^{19} cm^{-2} [6]. Moreover, authors of [5] have pointed out that the coloration intensity at the same fluences does not depend on the presence of dopands and impurities. On the other hand, it was stated in [16] that displacement defects induced by neutron irradiation increase the activity of impurities that participate in CC formation. In the 10^{18} to 10^{19} cm^{-2} neutron fluence range a shift of the 235 nm absorption band of Nd^{3+} into the long-wavelength region was observed [7]. This phenomenon was explained by local deformation of neodymium ion surrounding due to the creation of radiation defects. At neutron fluences of about 10^{19} cm^{-2} a saturation of induced absorption takes place [6], and at higher fluences an increase of the structural disorder was observed [6]. It was observed in [13, 17] in the form of amorphous microareas with size of about 10 nm. As it was determined, the annealing of radiation defects induced by neutron irradiation takes place in two steps. Colour centres created on radiation defects are destroyed at 670 to 870 K, and the radiation defects themselves are destroyed at temperatures 1200 to 1300 K [5, 16]. It indicates a diffusion mechanism of healing up of the radiation defects. After annealing at temperature 870 K, when radiation defects are not destroyed, new CCs on them may be easily created again under relatively soft irradiation (UV-light, X- or γ-rays).

$Gd_3Ga_5O_{12}$ The displacement defect formation in gadolinium gallium garnet (GGG) single crystals under electron and neutron irradiation was investigated in details in [1, 18 to 21]. Similar to YAG crystals in GGG crystals, with increase of the electron energy up to 3.5 MeV and increase of the radiation dose above 10^7 Gy (fluence $> 5 \times 10^{16}$ cm^{-2}) the induced changes of optical absorption spectra are observed, namely the absorption band at 33500 cm^{-1} [19] increases monotonously with irradiation dose. It is just what distinguishes these optical changes from other ones induced by γ-quanta and electrons with smaller energies and doses. The same band was observed in neutron-irradiated crystals of GGG, GGG:Nd and NGG (Nd$_3$Ga$_5$O$_{12}$) at fluences higher than 10^{16} cm^{-2} [18, 22]. Besides, the shift of the fundamental absorption

edge into the long-wavelength region with increasing irradiation dose was observed. The mentioned changes do not show a saturation tendency at electron fluences up to 10^{18} cm^{-2} and neutron fluences up to 10^{17} cm^{-2} [19]. On the base of peculiarities of accumulation kinetics and calculations of RDD concentration [1, 18, 23] the impact mechanism of radiation defect formation was considered to be responsible for these changes. The structural disordering process begins at neutron fluences higher than 10^{18} cm^{-2} [24, 25]. The annealing of induced defects is happening in two steps like in YAG crystals [21].

$Y_3Fe_5O_{12}$ Much efforts were spent to investigate the neutron irradiation influence on structural and magnetic properties of poly- and single crystals of yttrium iron garnet (YIG), related iron garnets [26 to 38] and epitaxial iron garnet films [1, 39, 40] as well. Essential changes of iron garnet parameters were observed by different authors at neutron fluences higher than 10^{18} cm^{-2}. At such fluences an increase of the crystal lattice parameter as well as a decrease of the saturation magnetization and Curie temperature take place. In a number of papers [35, 38, 39, 41] it was shown convincingly that a disordering process is responsible for these changes that occur as losing of long-range order in microareas that have been affected by the atom–atom displacement cascades. The rest bulk remains of the garnet structure. According to [41] this behaviour is common for crystals of garnet structure. Attempts to find out effects caused by the point displacement defects in iron garnet crystals were not successful under neutron irradiation with fluences of 10^{16} to 10^{17} cm^{-2}. This is due to the fact that the radiation defects with concentrations of about 10^{17} cm^{-3}, that can be relatively easily revealed by optical investigations in non-magnetic garnet crystals, cannot be observed in iron garnet crystals due to the masking effect of intensive absorption caused by the O^{2-}–Fe^{3+} charge transfer. Magnetic properties of iron garnet crystals in most cases are not sensitive enough to such concentration of point defects. Only in [42] the magnetooptical activity change was experimentally observed in Ga-substituted YIG epilayers after electron irradiation with energy of 3.5 MeV and fluence of 3×10^{18} cm^{-2}. It is unlikely caused by the irradiation induced disordering process and, on the other hand, it does not occur at smaller doses of irradiation when recharging is observed in other garnet crystals.

Ferrites with the spinel and magnetoplumbite structure   Many publications including several monographs (see [41, 43] and references therein) were devoted to the irradiation influence on ferrites with the spinel and magnetoplumbite structure. In [41] it was concluded that the crystal structure behaviour of these crystals is different from that mentioned above for garnet crystals at high neutron fluences. Especially, disordering in areas affected by atom displacement cascades does not lead to the loss of crystal ordering and results only in a redistribution of cations over unequivalent lattice sites.

LiNbO₃, KNbO₃, LiTaO₃   The oxygen atom displacement under electron irradiation in photorefractive crystals of LiNbO$_3$, KNbO$_3$ and LiTaO$_3$ was studied in [44 to 49]. The threshold displacement energy of oxygen atoms was experimentally determined. It was established that created colour centres are the metastable states of displacement defects after trapping of charge carriers. Thermal treatment at temperatures starting from 340 K leads to CC destroying, i.e. the carriers are getting free [46, 47]. After that CCs may be created again in the way of carrier trapping by existent RDDs due to ionizing effect of irradiation. Moreover, the CC formation rate in this case is much higher [46]. Destroying of radiation defects themselves takes place at temperature of about 600 K.

The neutron irradiation of the above crystals was virtually not studied. Only in [1, 18] the induced absorption spectra of lithium niobate crystals under the fast neutron irradiation with fluences of 10^{16} and 10^{18} cm^{-2} were examined.

YAlO$_3$ In [16] it is mentioned about the irradiation of yttrium aluminium perovskite crystals doped with neodymium (YAlO$_3$:Nd) by neutrons with fluences 10^{14} to 10^{19} cm^{-2}. Authors do not demonstrate absorption spectra of irradiated crystals, but note the presence of the same induced absorption bands as after γ-irradiation. Unlike the γ-irradiation, which leads to saturation of induced absorption at absorbed doses of 10^4 Gy, the induced absorption increases after neutron irradiation of YAlO$_3$:Nd crystals in proportion with neutron fluence.

Some works are devoted to the influence of high energy electrons and neutrons on oxide crystals as Li$_2$B$_4$O$_7$ [1], Bi$_{12}$SiO$_{20}$ [50], GdScO$_3$ [2]. The Li$_2$B$_4$O$_7$ single crystal possesses an interesting property, namely the stable CCs do not appear due to ionizing recharging of genetic defects. Induced coloration in this crystal arises only as a result of the RDD formation [1].

This work is devoted to further investigation of RDD and CC formation in complex oxide crystals under irradiation. The theoretical calculations of the cross-section value of the displacement process, the concentrations of displaced atoms and analysis of the RDD and CC accumulation kinetics in some complex oxide compounds are presented. New experimental results of irradiation of LiNbO$_3$ (LNO) crystals doped with transition metals (Fe and Cr) and YAlO$_3$ (YAP) crystals doped with Nd and Er as well are presented.

2. Theoretical Study

2.1 Calculation of cross-section of the displacement defect formation process and RDD concentration

During irradiation of complex compounds by high energy particles, i.e. in the case of ramified atom–atom collision cascades the role of atoms of different kinds in the RDD formation process in each sublattice must be taken into account [51]. The concentration of displaced atoms in the atom sublattice of the *j*-type created due to the initial displacement of one atom of the *i*-type with energy T_i can be expressed in the form

$$n_{d_{ij}} = n_i \int_{T_{d_i}}^{T_{\max_j}} \frac{d\sigma_{d_i}(E, T)}{dT} \, \nu_{ij}(T_i) \, dT_i \,, \tag{1}$$

where n_i is the concentration of *i*-atoms; $d\sigma_{d_i}/dT$ is the differential cross-section of the elastic scattering of irradiation particle on the atom of *i*-type that results in transfer of recoil energy T; $T_{\max}$ is the maximum possible recoil energy; T_d is the threshold displacement energy; $\nu_{ij}(T_i)$ is a cascade function, i.e. the number of displaced *j*-atoms per one initially knocked-out atom (IKA) of the *i*-type with energy T_i. The total concentration of displacements in *j*-sublattice during an irradiation by the time of dt will be expressed in the form

$$dn_{d_j} = \left(\sum_i n_{d_{ij}} \right) P \, dt = n_a \sigma_{d_j} \, d\Phi \,, \tag{2}$$

Table 1

The cross-section of the displacement formation process and the concentration per unit fluence of RDDs created in sublattices of some complex oxide crystals

crystal	atom	T_d (eV)	electrons (1.3 MeV)		electrons (3.5 MeV)		electrons (7 MeV)		fast reactor neutrons (~2 MeV)	
			σ_d (barn)	n_d/Φ (cm^{-1})	σ_d (barn)	n_d/Φ (cm^{-1})	σ_d (barn)	n_d/Φ (cm^{-1})	σ_d (barn)	n_d/Φ (cm^{-1})
Gd$_3$Ga$_5$O$_{12}$	Gd	66	0.01	0.001	4.92	0.413	10.32	0.867	22.86	1.92
	Ga	56	1.43	0.120	7.63	0.641	11.10	0.932	32.14	2.70
	O	40	8.41	0.706	15.30	1.285	25.04	2.103	231.6	19.45
Y$_3$Al$_5$O$_{12}$	Y	66	0.13	0.012	4.46	0.411	7.04	0.649	17.14	1.58
	Al	56	2.32	0.214	4.51	0.416	6.10	0.562	22.78	2.10
	O	40	8.62	0.795	16.55	1.526	25.55	2.356	158.6	14.62
Gd$_3$Sc$_2$Ga$_3$O$_{12}$	Gd	66	0.01	0.001	4.93	0.413	10.29	0.862	21.72	1.82
	Sc	56	0.78	0.065	2.35	0.197	3.47	0.291	15.63	1.31
	Ga	56	1.28	0.107	5.26	0.441	7.37	0.615	17.54	1.47
	O	40	8.35	0.700	15.43	1.293	24.64	2.069	207.8	17.41
Y$_3$Fe$_5$O$_{12}$	Y	66	0.12	0.010	4.57	0.386	7.46	0.630	25.47	2.15
	Fe	56	2.04	0.172	7.23	0.610	10.01	0.845	31.52	2.66
	O	40	8.28	0.699	15.84	1.337	26.03	2.197	211.5	17.85
YAlO$_3$	Y	66	0.20	0.016	7.34	0.578	11.16	0.919	30.33	2.39
	Al	56	2.31	0.182	4.52	0.356	6.17	0.486	26.40	2.08
	O	40	10.65	0.839	20.05	1.580	31.51	2.483	219.2	17.27
Y$_{0.5}$Er$_{0.5}$AlO$_3$	Y	66	0.11	0.009	3.69	0.291	6.00	0.473	15.10	1.19
	Er	66	0.01	0.001	4.14	0.326	8.69	0.685	11.55	0.91
	Al	56	2.32	0.183	4.48	0.353	6.08	0.479	25.63	2.02
	O	40	10.71	0.844	19.97	1.574	30.77	2.425	213.8	16.85
LiNbO$_3$	Li	5−25	2.38−12.55	0.180 −0.948	3.65−16.65	0.276−1.259	5.26−22.18	0.398−1.677	39.29−93.78	2.97−7.09
	Nb	25−125	0.001−1.20	0.0001−0.091	2.21−10.78	0.167−0.815	4.97−15.13	0.375−1.144	8.99−19.44	0.68−1.47
	O	53	7.13−7.25	0.539−0.548	13.11−13.76	0.991−1.040	20.08−22.02	1.518−1.665	152.4−159.3	11.52−12.04

where P is the fluence power; $d\Phi = P\,dt$ is the fluence of irradiation particles by the time of dt; $n_a = \sum n_i$ is the atom concentration in the crystal;

$$\sigma_{d_j} = \sum_i \left(q_i \int_{T_{d_i}}^{T_{\max_i}} \frac{d\sigma_{d_i}(E,T)}{dT} \, \nu_{ij}(T_i) \, dT_i \right)$$

is the total cross-section of the defect formation process in j-sublattice; $q_i = n_i/n_a$ is the relative concentration of i-atoms in polyatomic compound.

In the case of electron irradiation the approximate McKinley-Feschbach formula [52] was used for the RDD concentration calculation that describes the differential cross-section of Rutherford scattering of a relativistic electron in the Coulomb field of the point nucleus. In the case of fast neutron irradiation the elastic scattering of neutrons on nuclei of matter was described as scattering of hard spheres. In order to calculate the cascade functions the computer simulation of the atom–atom collision cascades was used. This procedure is based on the assumptions of the Kinchin-Pease binary collision model [53] and was described in details in [51].

The calculated cross-sections of the defect formation process and concentrations of displacements are presented in Table 1 for some crystals with garnet and perovskite-like structures. T_d values for ions of garnet and perovskite-like structure were assumed in calculations to be equal to the values for GGG atoms that have been estimated in [23]. The ionic radii for cations with different coordination positions were estimated from data of [54, 55] as average weighted values. The T_d values for oxygen ions of lithium niobate crystal were taken from [44, 45]. The threshold energy values for Nb and Li ions were varied in a wide range (from 25 to 125 eV for Nb) with saving its ratio to be equal to 5, which corresponds to the valence ratio for these ions in LNO crystal. The dependence of the displaced oxygen atom concentration on the electron irradiation energy in LNO is presented in Fig. 1. It is seen from the figure and from the Table 1 that the cation T_d value uncertainty has a weak influence on the estimation of the concentration of the oxygen RDD.

The observation that could be made from the calculation testifies that the RDDs are formed preferably in the oxygen sublattices of all complex oxide crystals considered.
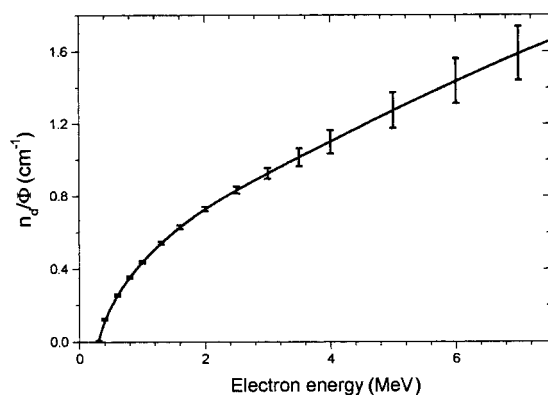
Fig. 1. Dependence of the displaced oxygen atom concentration in LNO crystal upon energy of electrons by irradiation

2.2 The accumulaton kinetics of RDD and CC

The CC accumulation kinetics in the case of ionizing recharging of genetic defects being present in a crystal is described by the differential equitation

$$\mathrm{d}n/\mathrm{d}t = (n_0 - n)\, P\sigma_{\mathrm{I}}\,, \tag{3}$$

where n_0 is the genetic defect concentration, σ_{I} is the cross-section of the genetic defect ionisation process. The solution of Eq. (3) with the initial condition of $n(0) = 0$ and the fluence power constant in a time has the form

$$n(\Phi) = n_0(1 - \mathrm{e}^{-\sigma_{\mathrm{I}}\Phi})\,, \tag{4}$$

and is plotted in Fig. 2 as the line 1.

The RDD generation in the simplest case is described by Eq. (2). Its solution with the initial condition of $n_{\mathrm{d}}(0) = n_0$ is the linear dose dependence

$$n_{\mathrm{d}}(\Phi) = n_0 + n_{\mathrm{a}}\sigma_{\mathrm{d}}\Phi\,, \tag{5}$$

presented in Fig. 2 as the line 2.

The probability of the Frenkel pair component to arise in a zone of instability of existing defects becomes quite considerable with the increase of the displacement concentration. It means that the further increase of defect quantity will be limited by the annihilation of displaced atoms on the existing vacancies. The probability to find oneself in the unstable zone may be estimated as the ratio of the total volume of unstable zones of all defects and the crystal volume. This probability is equal to $n_{\mathrm{d}}v_{\mathrm{r}}$ for crystal single volume, where v_{r} is the volume of the unstable zone of one radiation defect. The RDD accumulation limited by the annihilation process is described by the differential equation

$$\mathrm{d}n_{\mathrm{d}}/\mathrm{d}t = n_{\mathrm{a}} P\sigma_{\mathrm{d}}(1 - v_{\mathrm{r}}n_{\mathrm{d}})\,, \tag{6}$$

Fig. 2. Accumulation kinetics of radiation defects and colour centres: Curves 1 to 4 represent calculation after equations (4), (5), (7) and (9), respectively. The line 5 depicts the dependence $n_{\mathrm{d}}(\Phi) = n_{\mathrm{a}}\sigma_{\mathrm{d}}\Phi$

where the values of n_d, σ_d, ν_r corresponds to a certain sublattice. The solution of Eq. (6) at the initial condition of $n_d(0) = n_0$ is the dose dependence
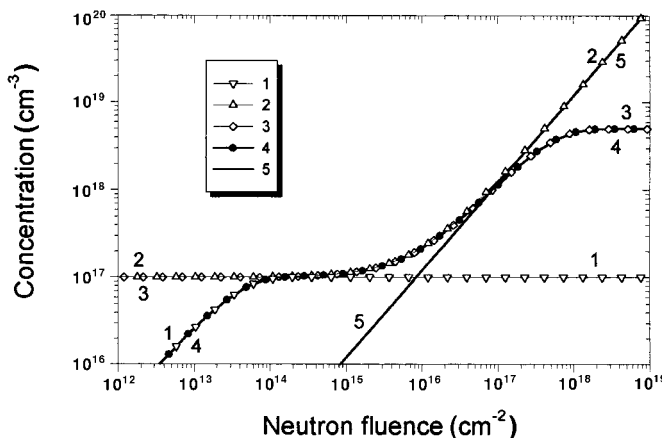
$$n_d(\Phi) = n_0\, e^{n_a\sigma_d\nu_r\Phi} + \frac{1}{\nu_r}\left(1 - e^{n_a\sigma_d\nu_r\Phi}\right), \tag{7}$$

drawn in Fig. 2 as line 3.

If the CC formation on RDDs takes place, then their accumulation kinetics is described by the differential equitation

$$dn/dt = (n_d - n)\,P\sigma_I. \tag{8}$$

Taking into account Eq. (7) and the initial condition $n(0) = 0$, the solution of the last equation is the dose dependence

$$n(\Phi) = \frac{1}{\nu_r}\left(1 - e^{-\sigma_I\Phi}\right) + \frac{\sigma_I(n_0\nu_r - 1)}{\nu_r(\sigma_I - n_a\sigma_d\nu_r)}\left(e^{n_a\sigma_d\nu_r\Phi} - e^{-\sigma_I\Phi}\right), \tag{9}$$

plotted in Fig. 2 as the line 4.

Since $\sigma_d \ll \sigma_I$, Eq. (9) can be simplified to Eq. (4) in the fluence range of $\Phi \ll 1/\sigma_I$ and to Eq. (7) when $\Phi \gg 1/\sigma_I$. In the region far from saturation due to the annihilation process, i.e. at $\Phi \ll 1/n_a\sigma_d\nu_r$, Eq. (7) simplifies to the linear dependence expressed by Eq. (5).

In general, there are two saturation regions of dose dependence for simple radiation defects and colour centres created on them. One of them takes place due to complete ionizing recharging of existing defects, and the other one is a result of annihilation of radiation defects when their concentration reaches a high level. In the second case the CC maximum concentration is defined as the inverse value of the instability zone volume.

3. Experiment Details

The samples been investigated were cut from single crystals grown by the Czochralski technique in the form of flat plates. The sample thickness was in the range of 0.5 to 2 mm. LNO:Cr crystals containing chromium of <0.02 wt% had a light green coloration. LNO:Fe crystal had a brown colour and contained 0.08 wt% of iron. Neodymium content in YAP:Nd crystal was about 1 at%. The YAP:Er crystal had the nominal composition $Y_{0.5}Er_{0.5}AlO_3$.

Irradiation by electrons with energy of 3.5 MeV was carried out in a channel of the LINAC linear accelerator by pulse beam with 1 mA average current. The frequency of electron pulses was 250 Hz, and the pulse duration was 4×10^{-6} s. The fluence power of a single pulse was 6.24×10^{13} cm^{-2} s^{-1}. The irradiation was carried out up to 10^{16} cm^{-2} integral fluence, that corresponds to absorbed dose of about 2×10^6 Gy.

The neutron and γ-quanta irradiations were done in the IRT-5000 research nuclear reactor (Institute of Physics of the Latvian Academy of Science). The reactor γ-contour was a source of γ-quanta with energy of 1.1 MeV. The γ-irradiation was carried out up to 8×10^5 Gy absorbed dose. The power of absorbed dose was about 10 Gy s^{-1}. The neutron irradiation was performed in the VEK-8 vertical channel. The power of fast neutron fluence was of 2.6×10^{12} cm^{-2} s^{-1}. The accompanying γ-irradiation had the absorbed dose power of about 200 Gy s^{-1}. Irradiation by the mixed γ-neutron radiation

was performed at the fast neutron fluence of 10^{14} to 5×10^{18} cm^{-2}. The sample temperature did not exceed 330 K during the γ- and electron irradiations and 310 K during the neutron irradiation.

The absorption spectra were registered by the spectrophotometer Specord M-40 (Carl Zeiss Jena) in the wavelength region of 200 to 900 nm. The reflection losses were not taken into account. The induced absorption was determined as the difference between absorption coefficients after and before irradiation.

4. Results and Discussion

4.1 Lithium niobate

The fast reactor neutron irradiation of LNO:Cr and LNO:Fe crystals leads to the induced absorption in the visible range of the spectrum (see Fig. 3a and b). The AA is similar to that induced by γ-quanta and electrons [1, 44 to 47, 56]. At present there is no common opinion on the CC nature and their creation mechanisms in LNO crystals irradiated by γ-quanta or electrons. Different models of CC were considered [44 to 47, 56]: F-type centres; a transition of niobium ions to a lower valent state; hole centres O$^-$ localized near cation sublattice defects; bipolarons; recharging of doping ions, and complex associates consisting of an oxygen vacancy and impurity. It should be pointed that the role of different impurities in the formation of optical and paramagnetic centres in LNO and LNO:Mg under low temperature γ-irradiation was investigated in details in [57 to 59].

The induced absorption spectra after the irradiation by γ-quanta ($E_\gamma = 1.1$ MeV, $D = 8 \times 10^5$ Gy) and electrons ($E_e = 3.5$ MeV, $\Phi = 10^{16}$ cm^{-2}, $D = 3 \times 10^6$ Gy) for the same crystals are presented in Fig. 3c. The similar absorption structure testifies an identical nature of CCs induced by radiation of various kinds, although the absorption intensity after the neutron irradiation reaches much higher values. Moreover, the widening of the short-wavelength absorption edge takes place at higher doses of the neutron irradiation. The latter was observed in pure LNO also [1].

The induced absorption spectra of LNO:Cr and LNO:Fe crystals after irradiation of all types are somewhat different. This may be caused by a difference in CC formation process due to the presence of impurities of different types. This problem was investigated in [1, 46, 47, 57 to 59].

There are some distinctions in the induced absorption behaviour for LNO:Cr and LNO:Fe crystals at higher neutron fluences. The dose dependencies of the induced absorption for wavelength of 475 nm (21050 cm^{-1}) are presented in Fig. 4. The induced absorption in LNO:Cr crystal in a maximum reaches the value about 1.5 cm^{-1} already at fluence 10^{14} cm^{-2}, and remains practically the same in the fluence range 10^{14} to 10^{16} cm^{-2}. In the case of LNO:Fe crystal the induced absorption is practically imperceptible in the fluence range 10^{14} to 10^{15} cm^{-2}.

Under the irradiation by γ-quanta and electrons the additional absorption arises as a result of CC formation due to the ionisation of genetic defects [1]. Its maximum level is reached when all genetic defects are recharged or the CC creation–destroying equilibrium is arrived. As a rule this occurs at 10^3 to 10^5 Gy absorbed doses that corresponds to fluences of $5 \times (10^{12}$ to $10^{14})$ cm^{-2} for electron irradiation with energy of 3 to 5 MeV [1]. So, the AA presented in Fig. 3c conforms approximately with the saturation of the ionizing recharging process. It should be noted that the induced AA disappears after
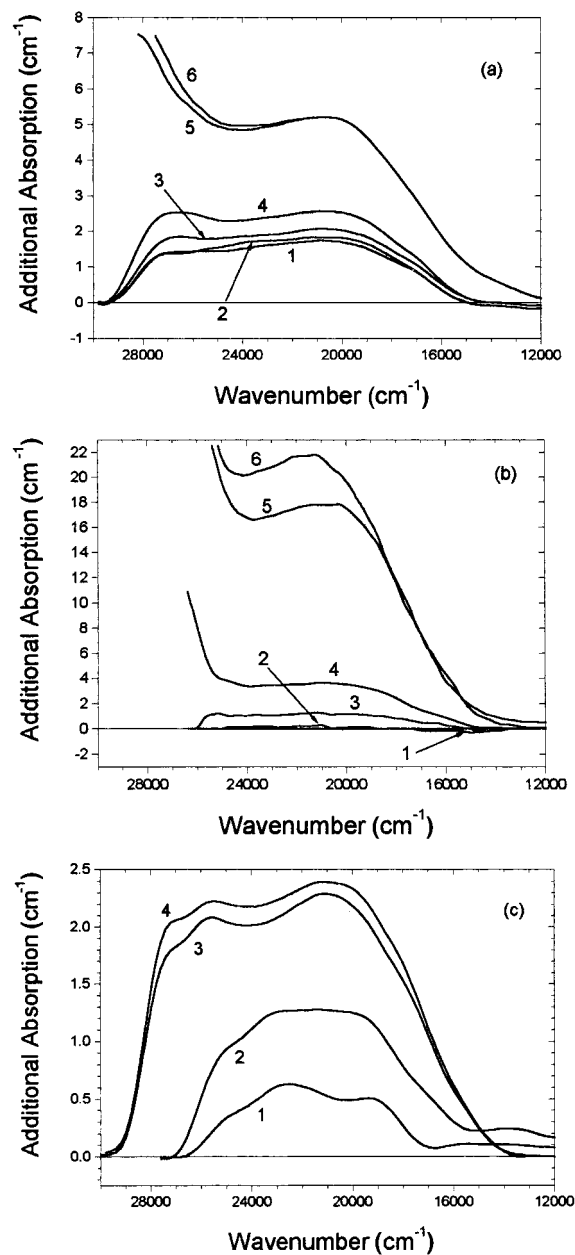
Fig. 3. The AA spectra of a) LNO:Cr and b) LNO:Fe crystals irradiated by fast reactor neutrons with fluences 10^{14} (1), 10^{15} (2), 10^{16} (3), 10^{17} (4), 10^{18} (5) and 5×10^{18} cm^{-2} (6). Fig. 3c represents the AA spectra of LNO:Fe (1,2) and LNO:Cr (3,4) crystals irradiated by γ-quanta (1,4) with absorbed dose 0.8 MGy and electrons (2,3) with energy 3.5 MeV and fluence 10^{16} cm^{-2} (absorbed dose 2 MGy)

annealing in air at 470 K in LNO:Cr crystal and above 670 K for LNO:Fe crystal. The latter shows that the CC thermal stability in LNO:Fe crystals is higher.

The RDD formation process becomes remarkable at increased doses of high energy irradiation and it is responsible for the AA rise at much higher fluences of irradiation [1, 44, 45]. The ionizing processes at neutron irradiation also take place due to braking of secondary particles (the knocked-out atoms with energy higher than an ionisation

Fig. 4. The dose dependencies of AA in neutron irradiated crystals in a) semi-logarithmic and b) double logarithmic scales. The dose dependencies of AA induced by irradiation at wavelength 475 nm are presented by the curves 1,4 and 5 (5 is the absorption above the level at fluence $10^{14}\,cm^{-2}$) in LNO:Cr and by the curves 2,3 in LNO:Fe. The dose dependence of AA at 300 nm in GGG is shown by the curve 6 for comparison

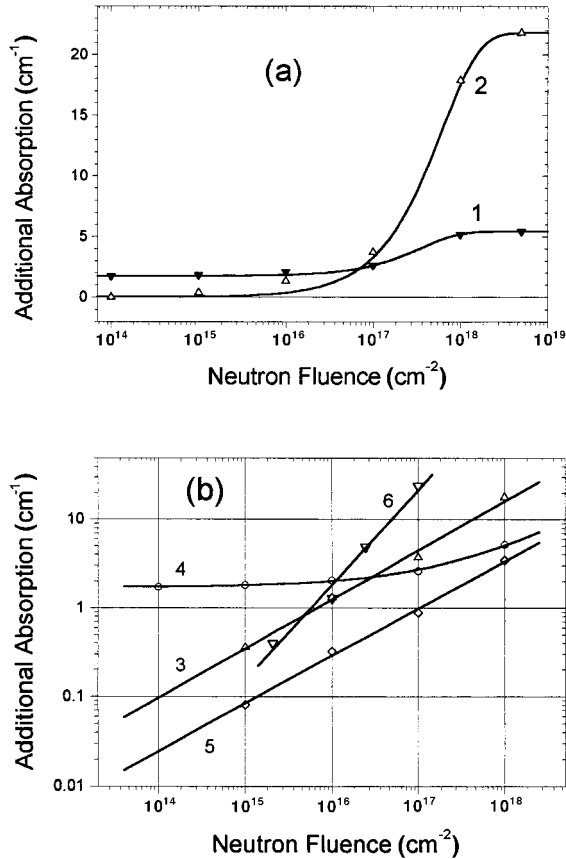threshold). Moreover, the reactor neutron radiation is always accompanied by γ-radiation. Thus, the presence of induced absorption in LNO:Cr crystal already at $10^{14}\,cm^{-2}$ fluence must be obviously associated with an ionisation of genetic defects, since, according to our calculations, the RDD concentration at such fluence is too small ($\sim 10^{15}\,cm^{-3}$). At that the value of this absorption is approximately equal to the AA saturation level at the ionizing recharging after γ- and electron irradiation. The RDD concentration at neutron fluences of 10^{16} to $10^{18}\,cm^{-2}$ reaches an essential value and the RDD formation is responsible for the AA rise. In the case of LNO:Fe crystal the AA is not observed at neutron fluences up to $10^{15}\,cm^{-2}$. The induced absorption in this crystal after the 'soft' irradiation (see Fig. 3c) is considerably lower than in LNO:Cr crystal at the same irradiation dose. On the other hand, the AA intensity in LNO:Fe crystal at fluences of 10^{16} to $10^{18}\,cm^{-2}$ is somewhat higher than in LNO:Cr crystal.

Let us discuss the dose dependencies of the induced absorption rise presented in Fig. 4 for both LNO:Cr and LNO:Fe crystals after neutron irradiation. As it is seen from Fig. 4a the induced absorption has the saturation tendency at fluences $\Phi > 10^{18}\,cm^{-2}$ in both crystals, that may be explained by the defect annihilation when their concentration reaches a considerable value. Taking into account the estimation of the total cross-section of the displacement formation process obtained in Section 2.1, the approximation of $\Delta\alpha(\Phi)$ dose dependencies by Eq. (7) may be done (solid lines 1

Ta b l e 2

The instability zone dimension estimations obtained from approximation of dose depen-
dencies shown in Fig. 4a: V and R are zone volume and its radius; N is the number of
atoms inside the zone

crystal	V (10^{-19} cm^3)	R (nm)	N
LNO:Fe	1.42	3.24	2700
LNO:Cr	2.35	3.83	4500

and 2 in Fig. 4a). It allows to estimate the size of zones of radiation defect instability in
LNO crystals. Values of the average volume V of instability zones, their radii R (with
assumption of spherical form of zone) and the quantity of crystal atoms N inside of
instability zone are presented in Table 2 for LNO:Fe and LNO:Cr crystals.

The dose dependencies in double logarithmic scale at $\Phi < 10^{18}$ cm^{-2} are presented in
Fig. 4b. Here the lines 3 and 4 represent the dose dependencies for LNO:Fe and
LNO:Cr crystals, respectively, and the line 5 represents the induced absorption rise
above the absorption level of LNO:Cr crystal at 10^{14} cm^{-2} fluence. The lines 3 and 5
are approximations of dose dependencies by Eq. (5). As it is seen from the figure the
line is a good approximation for this case. The dose dependencies for two LNO crystals
differ one from another only by a parallel shift.

The RDD formation rate at fluence $\Phi < 10^{18}$ cm^{-2} may be considered as a constant
one. It is determined by the concentration of crystal atoms and the total cross-section
of the atom displacement process for each sublattice (2). The latter is determined by
the threshold displacement energy T_d, differential cross-section of the energy transfer
process and the cascade function (see Eq. (1)). All above-mentioned parameters are
determined by the main crystal content and cannot depend significantly on the pre-
sence of dopants. In optical absorption spectra both RDD or CCs formed on them may
manifest themselves due to recharging or the complex formation. In the first case the
concentrations of active optical centres must be equal for both LNO crystals. That is
why we conclude that CCs responsible for absorption induced by neutron irradiation
are formed during the secondary processes with RDD participation. The same conclu-
sion was made in [46] as a result of studies of the destroying of radiation defects and
induced CCs by annealing.

The concentration of CCs formed during each particular process depends on its prob-
ability, i.e. on its cross-section. The intensity of induced absorption in the maximum of
an appropriate band is proportional to the concentration of the corresponding CCs and
to the oscillator strength of the optical transition. If we assume that the absorption at
475 nm is associated with CCs of the same type, then the difference in dose dependen-
cies for investigated crystals may be explained by different cross-sections of the same
CC formation process or different oscillator strengths caused by the dopant. The alter-
native explanation may be based on the assumption that different CCs in the same
spectral region are formed in LNO crystals with different dopants. Thus the presence of
impurities may strongly affect the CC formation process in LNO crystal though the
RDDs are created in the crystal matrix mainly. In this relation it deserves mentioning
that the presence of impurities may dramatically change the character of the defect
centre formation process, as it was shown in LNO:Fe and LNO:Mg,Fe [58] subjected to
γ-irradiation.

The slope of the dose dependencies in the double logarithmic scale (Fig. 4b) is an additional peculiarity of the induced absorption in LNO:Fe and LNO:Cr crystals. The change of scale factor before variables when taking the logarithm of the $\Delta\alpha(\Phi)$ dependence leads only to the parallel shift of the dependence, but the slope gives an information about the type of the CC accumulation kinetics. The CC formation process may be considered as a quasi-chemical reaction. The estimation of the slope of the kinetic curve in coordinates $\ln(dC/dt)$ versus $\ln(C)$, where C is the concentration of the component taking part in reaction, is a common determination method for the order of a chemical reaction. However, there is a complication during the experimental data processing due to the low accuracy of the numerical differentiation of a function presented in table form. To find the reaction order we have used the linear approximation of the dependence $\lg(\Delta\alpha)$ versus $\lg(\Phi)$ at low fluences ($\Phi \leq 10^{18}$ cm^{-2}),

$$\lg(\Delta\alpha) = A \lg(\Phi) + B, \tag{10}$$

where A and B are the approximation parameters defined by the least squares method. Taking into account that $\Delta\alpha$ value is proportional to the CC concentration n_c, Eq. (10) may be transformed to the form

$$\lg(n_c) = A \lg(\Phi) + B'. \tag{11}$$

From Eq. (11) the functional dependencies $n_c(\Phi)$ and $\Phi(n_c)$ may be easily derived. Differentiating the first of them with respect to Φ and substituting the second one to the obtained expression one can obtain the following dependence:

$$\lg(dn_c/d\Phi) = \frac{A-1}{A} \lg(n_c) + \frac{B'}{A} + \lg(A), \tag{12}$$

from which the quasi-chemical reaction order has the form

$$N = \frac{A-1}{A}. \tag{13}$$

Then the kinetics of the CC concentration change is described in the form

$$\frac{dn_c}{d\Phi} = Kn_c^N, \tag{14}$$

where K is the reaction rate constant.

The results of the approximation of dose dependencies plotted in Fig. 4b (lines 3, 5, 6) and the orders of the CC formation quasi-chemical reactions are presented in Table 3. The dose dependence of the induced absorption in GGG crystal at wavelength 300 nm ($\sim$33300 cm^{-1}) after neutron irradiation as a result of the RDD formation [18] is presented in Fig. 4b (line 6) for comparison. As it is seen from Table 3 the reaction

Table 3
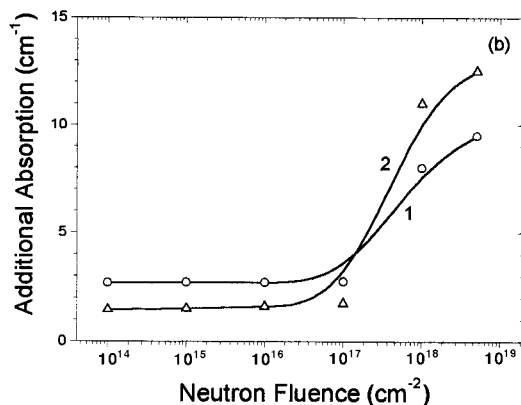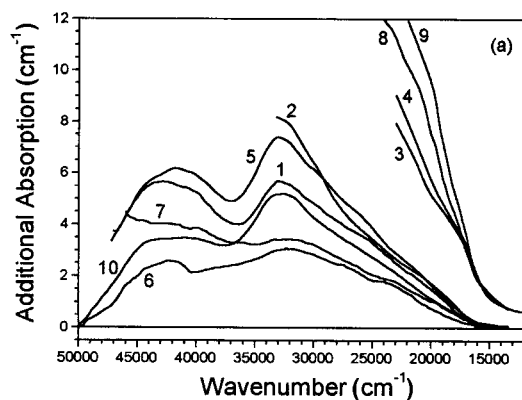The results of linear approximation of dependence $\lg(\Delta\alpha)$ versus $\lg(\Phi)$ shown in Fig. 4b and the estimations of the quasi-chemical reaction order $N = 1 - 1/A$

crystal		A	B	$N = 1 - 1/A$
LNO:Fe	(curve 3)	0.554	-8.97	-0.803
LNO:Cr	(curve 5)	0.533	-9.12	-0.802
GGG	(curve 6)	1.074	-16.9	0.069

orders for both LNO crystals are practically the same, that indicates the similarity of
the CC formation processes for the crystals under investigation. The reaction order for
GGG crystal is very close to zero, that corresponds to the quasi-chemical reaction with
constant velocity. Similar observations were done in [60] on corundum crystal irradia-
tion. Such kinetics can describe the CC accumulation in the case of the CC formation
directly on single RDDs that are created according to Eq. (5) with constant rate (see
line 5 in Fig. 2). Quite different situation is observed in LNO:Fe and LNO:Cr crystals
in which the rate of the CC concentration change decreases at concentration increasing
in form of $dn_c/d\Phi \approx K/n_c^{0.8}$. This dependence indicates decreasing of the cross-section
of the CC formation process with the increase of their concentration. The performed
investigations do not allow us to point out a reason of such behaviour of the AA dose
dependencies in LNO crystals. Nevertheless, one can assume that such behaviour is a
result of the Debye-Hückel screening effect [61] during the charged defect interaction,
that leads to decreasing of its ionisation cross-section with increasing defect concentra-
tion.

4.2 Yttrium aluminium perovskite

The irradiation of YAP:Nd and YAP:Er crystals by fast neutrons with fluences 10^{14} to
10^{17} cm^{-2} leads to the induced absorption (Fig. 5a) in UV- and visible region of spec-
trum (50000 to 15000 cm^{-1}) with maxima at 42000, 33000, 23000 and 20000 cm^{-1}. The AA spectra of YAP crystals of the same structure and intensity are observed after γ-irradiation with dose 8×10^5 Gy and the electron irradiation (3.5 MeV) with fluence of 10^{16} cm^{-2} (absorbed dose about 2×10^6 Gy). The latter two are practically coincident one with another for each of crystals. That is why only spectra after electron irradiation are plotted in the figure. The AA intensity weakly depends on irra-

Fig. 5. a) The AA spectrum of YAP:Nd (1 to 5) and YAP:Er (6 to 10) crystals irradiated by fast reactor neutrons with fluence 10^{15} (1,6), 10^{17} (2,7), 10^{18} (3,8) and 5×10^{18} cm^{-2} (4,9) and by electrons with energy $E_e = 3.5$ MeV and fluence 10^{16} cm^{-2} (5,10) and b) the dose dependencies of AA at wavelength 435 nm (23000 cm^{-1}) in YAP:Nd (1) and YAP:Er (2) crystals after neutron irradiation

diation dose 10^5 to 10^7 Gy absorbed doses of γ-quanta or on the neutron fluence in the range 10^{14} to 10^{17} cm^{-2}. The similar structure of the AA indicates the same nature of CCs created in YAP crystals under irradiation of various kinds (γ-quanta, electrons and neutrons) with doses mentioned above. It should be noted that the intensity of the AA induced by neutron irradiation in this range is somewhat lower than the AA level after irradiation by γ-quanta or electrons.

Iron ions are known to be the most common impurity in YAP crystals and they can exist in the valence states Fe^{2+} and Fe^{3+} [62]. The Fe^{2+} ions are considered to be responsible for the intensive absorption at 43000 cm^{-1} and the weak one at 32000 cm^{-1}. During the irradiation the reactions of $O^{2-} + h\nu \rightarrow O^- + e^-$ and $Fe^{3+} + e^+ \rightarrow Fe^{2+}$ take place that result in the appearance of the AA maxima of 42000 and 33000 cm^{-1} [62, 63].

The AA bands at 23000 and 20000 cm^{-1} are assumed to be associated with the hole center O^- located close to cation vacancy and F-type centres [63, 64]. There are two non-equivalent positions of oxygen ions in YAP structure [65] and consequently, two types of energy non-equivalent F- and O^- centres can be formed. The F-centres with absorption band in the range of 20000 to 24000 cm^{-1} have been observed in other irradiated crystals with garnet and perovskite-like structure [66].

The annealing in air of γ-irradiated crystals leads to the AA intensity decrease at temperatures above 470 K and to the complete AA disappearing in YAP:Er crystal at $T \sim 1000$ K, while the AA in YAP:Nd crystal remains practically unchanged at this temperature.

The AA intensity grows rapidly and the broadening of the short-wavelength absorption edge takes place at fluence 10^{18} cm^{-2} of neutron irradiation (Fig. 5a). It indicates an appearance in irradiated crystals of new radiation defects. The concentration of the displacement defects at 10^{18} cm^{-2} neutron fluence is about 2×10^{19} cm^{-3} and oxygen vacancies are the main part of them. So, the RDDs in the oxygen sublattice should be responsible for the revealed AA growth. At neutron fluence $\sim 5 \times 10^{18}$ cm^{-2} the saturation of the RDD formation process begins as it was observed also in LNO crystals. Due to the high optical density of studied samples we could not separate the maxima in the AA spectra. The dose dependencies of induced absorption in YAP crystals at neutron irradiation obtained at 23000 cm^{-1} are presented in Fig. 5b. It should be pointed that the AA intensity is higher in YAP:Nd crystals after irradiation with the 10^{14} cm^{-2} neutron fluence than in YAP:Er crystals, but the reverse behaviour is observed at fluence 10^{18} cm^{-2} when the RDDs are formed. Like in LNO crystals it testifies that the dopant presence can play an important role in the CC formation because the RDD concentration is almost the same in both studied YAP crystals.

5. Conclusions

The analysis of published data on RDD formation in complex oxide crystals reveals some overall traits in this phenomenon. It allows to consider this process from a single point of view and to use the relatively simple general models describing the RDD creation and their accumulation. On the other hand, the effects being observed in the change of crystal properties are defined not only by RDD formation but also by secondary processes of mutual influence of created RDDs, impurities and structural imperfections of crystal under irradiation.

The carried out calculations of the RDD concentration in crystals of complex oxides testify that they are formed most effectively in the oxygen sublattice in practically all studied crystals. Their concentration is large enough to reveal them by optical spectroscopy methods after neutron irradiation with fluence about 10^{17} cm^{-2} or, for example, after electron irradiation with energy 3.5 MeV and fluence of about 10^{18} cm^{-2}. These results agree well with published data on displacement defects in various transparent crystals with garnet and perovskite-like structure. The process of single displacement defect formation saturates at neutron fluence higher than 10^{18} cm^{-2}. Exactly the same behaviour was found in the LNO:Cr, LNO:Fe, YAP:Nd and YAP:Er crystals subjected to irradiation by fast reactor neutrons. The performed analysis of accumulation kinetics of CCs formed on growth and radiation defects shows that in general case there are two regions of saturation. The first of them takes place at lower fluences and corresponds to saturation of the genetic defect recharging process. The second one occurs at higher fluences and conforms with equilibrium between processes of the RDD formation and annihilation of their components. The expressions obtained from the analysis allow to describe satisfactorily the dose dependencies obtained experimentally for LNO crystals and to obtain an estimation of the instability zone dimensions for RDD.

The created RDDs participate in the formation of optically active colour centres as well as the growth defects and impurities at lower doses of irradiation. The comparison of the absorption induced by neutron irradiation in the LNO and YAP crystals with the AA induced by γ-irradiation or relative low doses of electrons confirms that practically the same CCs are formed in both cases. This distinguishes these crystals from such ones as $Gd_3Ga_5O_{12}$ and $Li_2B_4O_7$. At the same time there are some peculiarities in the CC formation processes in each type of crystal. In particular the maximum level of AA induced by the growth defect recharging is somewhat lower in all cases after neutron irradiation, and it is practically absent in the LNO:Fe crystals at neutron fluence less than 10^{15} cm^{-2}. The comparison of the behaviour of crystals with different impurity contents testifies that their AA caused by the RDD formation can differ significantly in its intensity. Nevertheless, its structure remains generally the same. This fact can suggest that the CC formation proceeds in secondary processes that are significantly affected by impurity presence. The difference in dimensions of the Frenkel pair annihilation zone in the LNO:Cr and LNO:Fe crystals and different thermal stability of CCs also suggest this explanation.

In the LNO:Cr and LNO:Fe crystals it was found that the CC accumulation decelerates with neutron fluence increase according to the law: $dn_c/d\Phi \approx K/n_c^{0.8}$. It distinguishes the LNO crystal behaviour from other oxide crystals, for example, such as GGG and corundum. It is supposed that the cross-section decrease of the defect ionisation process with the RDD concentration rise, i.e. an effect like the screening effect of Debye-Hückel, may be responsible for this behaviour.

References

[1] A.O. MATKOVSKII, D.YU. SUGAK, S.B. UBIZSKII, O.I. SHPOTIUK, E.A. TSHORNYI, M.M. VAKIV, and V.A. MOKRITSKII, Influence of ionizing radiation on materials of electronic engineering, Izd. Svit, Lviv 1994 (in Russian).

[2] Z.T. Azamatov, P.A. Arsenev, H.S. Bagdasarov, I.R. Bedilov, A.A. Evdokimov, and V.I. Tsehanovich, Defects in quantum electronics materials, Izd. Fan, Tashkent 1991 (in Russian).

[3] N.A. Mironova and U.A. Ulmanis, Radiation defects and iron group metals in oxides, Izd. Zinatne, Riga 1988 (in Russian).

[4] Sh.A. Vahidov and A.A. Yusupov, Izv. AN Uzb. SSR, Ser. Fiz. i mat. nauk **1**, 70 (1973) (in Russian).

[5] Sh.A Vahidov, E.M. Ibragimova and B. Kaipov, in: Radiation effects in some laser crystals, Izd. Fan, Tashkent 1977 (p. 50) (in Russian).

[6] F.A. Zaitov, N.N. Litvinova, V.G. Savitskii, and V.G. Sredin, Irradiation resistance in optoelectronics, Ed. V.G. Sredin, Izd. Voenizdat, Moscow 1987 (in Russian).

[7] P.K. Habibullaev, I.R. Bedilov, and H.B. Beysembayeva, Radiation stimulated processes in optical quantum generators, Izd. Fan, Tashkent 1977 (in Russian).

[8] J.M. Bunch, Phys. Rev. B **16**, 724 (1977).

[9] I.R. Bedilov and H.B. Beysembayeva, Ukr. Fiz. Zh. **25**, 1853 (1980) (in Russian).

[10] R.R. Atabekian, V.A. Gevorkian, A.H. Grigorian, G.N. Eritsian, R.K. Ezoian, and V.H. Sarkisov, Izv. AN Arm. SSR, Ser. Fizika **15**, 306 (1980) (in Russian).

[11] M.R. Bedilov, P.K. Habibullaev, and H.B. Beysembayeva, Zh. Tekhn. Fiz. **51**, 2436 (1981) (in Russian).

[12] A.F. Rakov, phys. stat. sol. (a) **76**, K57 (1983).

[13] G.I. Natsvlishvili and R. Verner, Izv. AN USSR, Ser. Fizika **48**, 266 (1984) (in Russian).

[14] M.R. Bedilov, H.B. Beysembayeva, P.K. Habibullaev, and R.P. Saidov, Ukr. Fiz. Zh. **31**, 59 (1986) (in Russian).

[15] K. Chakrabarti, J. Phys. Chem. Solids **49**, 1009 (1988).

[16] Sh.A. Vahidov, B. Esemuratov, E.M. Ibragimova, and A.F. Rakov, in: Radiation stimulated effects in oxygen crystals and glasses, Izd. Fan, Tashkent 1977 (p. 80) (in Russian).

[17] G.I. Natsvlishvili and P. Werner, Electron Microscopy, Proc. 10th Internat. Conf., 1982, Vol. 2 (p. 49).

[18] S.B. Ubizskii, A.O. Matkovskii, D.Yu. Sugak, R.M. Kholyavka, U.A. Ulmanis, L.E. Vitruk, V.I. Litvinenko, and B.M. Kopko, Izv. AN Latv. SSR, Ser. Fiz. i tekhn. nauk **6**, 12 (1989) (in Russian).

[19] A.O. Matkovskii, D.Yu. Sugak, S.B. Ubizskii, U.A. Ulmanis, and A.P. Shakhov, phys. stat. sol. (a) **128**, 21 (1991).

[20] A.O. Matkovskii, D.Yu. Sugak, S.B. Ubizskii, and I.V. Kityk, Rad. Effects and Defects in Solids **133**, 153 (1995).

[21] A.O. Matkovskii, D.Yu. Sugak, S.B. Ubizskii, and I.V. Kityk, Optoelectronics Rev. **2**, 41 (1995).

[22] A.O. Matkovskii, I.M. Solskii, D.Yu. Sugak, B.M. Kopko, E.A. Tshornyi, and V.I. Litvinenko, in: Radioelectronic materials science, Chap. III, Lviv, 1991 (p. 68) (in Russian).

[23] Ya. Dovgii, I. Kityk, A. Matkovskii, D. Sugak, and S. Ubizskii, Soviet Phys. − Solid State **34**, 575 (1992).

[24] M.M. Brezgunov and A.N. Karpov, Izv. AN Latv. SSR, Ser. Fiz. i tekhn. nauk **5**, 18 (1990) (in Russian).

[25] Yu. Chukalkin and V.R. Shtirts, phys. stat. sol. (a) **144**, 9 (1994).

[26] A.K. Podsekin and V.A. Sarin, Voprosy atomnoy nauki i tekhniki, Ser. Fiz. rad. povr. i rad. materialov **4**, No. 23, 84 (1982) (in Russian).

[27] A.K. Podsekin, V.N. Zaytsev, and S.P. Solovyov, Voprosy atomnoy nauki i tekhniki, Ser. Fiz. rad. povr. i rad. materialov **4**, No. 23, 86 (1982) (in Russian).

[28] A.K. Podsekin and V.A. Sarin, Soviet Phys. − Techn. Phys. **26**, 586 (1981).

[29] A.K. Podsekin and V.N. Zaytsev, Soviet Phys. − Solid State **23**, 160 (1981).

[30] A.K. Podsekin and V.N. Zaytsev, Soviet Phys. − Solid State **24**, 342 (1982).

[31] A.K. Podsekin, V.N. Zaytsev, and I.I. Kuzmin, Soviet Phys. − Techn. Phys. **27**, 54 (1982).

[32] I.I. Brezgunov and A.A. Petrov, Ukr. Fiz. Zh. **34**, 616 (1988) (in Russian).

[33] H. Pascard, Phys. Rev. B. **30**, 2299 (1984).

[34] H. Pascard, Phys. Rev. B. **33**, 7252 (1986).

[35] H. Pascard, A. Globus, G. Roult, and P. Bacher, Am. Ceram. Soc. Bull. **66**, 813 (1987).

[36] J.M. Greneche, H. Pascard, and J.R. Regnard, Solid State Commun. **65**, 713 (1988).

[37] S.V. Sinitsin, A.N. Spirin, and M.N. Uspensky, Hyperfine Interaction **29**, 1217 (1986).

[38] Yu.G. Chukalkin, V.R. Shtirts, and B.N. Goshchitskij, phys. stat. sol. (a) **79**, 361 (1983).

[39] S.B. Ubizskii, A.O. Matkovskii, R.M. Kholyavka, and M.M. Rak, J. Magn. Magn. Mater. **125**, 110 (1993).

[40] R.Ya. Kemers, L.M. Korenkova, T.N. Letova, I.M. Sarayeva, and U.A. Ulmanis, Izv. AN Latv. SSR, Ser. Fiz. i tekhn. nauk **4**, 28 (1988) (in Russian).

[41] B.N. Goshchitskii, A.N. Men, I.A. Sinitskii, and Yu.G. Chukalkin, Structure and magnetic properties of oxygen magnetics irradiated by fast neutrons, Izd. Nauka, Moscow 1986 (in Russian).

[42] S.B. Ubizskii, A.O. Matkovskii, and M. Kuzma, J. Magn. Magn. Mater. **157/158**, 279 (1996).

[43] U.A. Ulmanis, Radiation phenomena in ferrites, Energoatomizdat, Moscow 1984 (in Russian).

[44] E.R. Hodgson and F. Agulló-López, Solid State Commun. **64**, 965 (1987).

[45] E.R. Hodgson and F. Agulló-López, Nuclear Instruments Methods in Phys. Res. B **32**, 42 (1988).

[46] E.R. Hodgson and F. Agulló-López, J. Phys.: Condensed Matter **1**, 10015 (1989).

[47] E.R. Hodgson and F. Agulló-López, J. Phys.: Condensed Matter **3**, 285 (1991).

[48] E.R. Hodgson, C. Zaldo, and F. Agulló-López, Solid State Commun. **75**, 351 (1990).

[49] E.R. Hodgson and F. Agulló-López, Radiation Effects and Defects in Solids **119/121**, 891 (1991).

[50] E.R. Hodgson, L. Arizmendi, and F. Agulló-López, Nuclear Instruments Methods in Phys. Res. B **65**, 275 (1992).

[51] S.B. Ubizskii, Visnyk Derzhavnoho Universytetu Lvivska Politechnika **357**, 88 (1998) (in Ukrainian).

[52] W.A. McKinley and H. Feschbach, Phys. Rev. **74**, 1759 (1948).

[53] G.W. Kinchin and R.S. Pease, Rep. Progr. Phys. **18**, 1 (1955).

[54] G.B. Bokiy, Crystal chemistry, Izd. Nauka, Moscow 1971 (in Russian).

[55] R.D. Shannon, Acta Cryst. A **32**, 751 (1976).

[56] O.F. Schirmer, O. Thiemann, and A. Wohlecke, J. Phys. Chem. Solids **52**, 185 (1991).

[57] G. Corradi, K. Polgár, I.M. Zaritskii, L.G. Rakitina, and N.I. Deriugina, Soviet Phys. – Solid State **31**, 1542 (1989).

[58] I.M. Zaritskii, L.G. Rakitina, G. Corradi, K. Polgar, and A.A. Bugai, J. Phys.: Condensed Matter **3**, 8457 (1991).

[59] I.M. Zaritskii, L.G. Rakitina, and K. Polgár, Soviet Phys. – Solid State **37**, 1970 (1995).

[60] P. Levy, Phys. Rev. **123**, 1226 (1961).

[61] F. Agulló-López, C.R.A. Catlow, and P.D. Townsend, Point Defects in Materials, Academic Press, New York 1988 (p. 34).

[62] J. Kvapil, Jos. Kvapil, I. Kubelka, and R. Futrara, Cryst. Res. Technol. **18**, 27 (1983).

[63] A. Matkovski, A. Durygin, A. Suchocki, D. Sugak, G. Neuroth, F. Wallrafen, V. Grabovski, and I. Solski, Optical Mater. **12**, 75 (1999).

[64] A. Riabov, N. Stelmach, V. Sorokin, G. Yermakov, and G. Akkerman, Neorg. Mater. **28**, 178 (1992).

[65] L. Vasylechko, L. Akselrud, A. Matkovski, D. Sugak, A. Durygin, Z. Frukacz, and T. Lukasiewicz, J. Alloys Compounds **242**, 18 (1996).

[66] A. Matkovski, A. Durygin, A. Suchocki, D. Sugak, F. Wallrafen, and M. Vakiv, Radiation Effects and Defects in Solids, to be published.